OBSERVATIONS OF THE QUADRUPOLAR OSCILLATIONS AT GSI SIS-18

R. Singh, P. Forck, P. Kowina, GSI, Darmstadt, Germany
W.F.O. Müller, J.A. Tsemo Kamga, T. Weiland, TEMF, Technische Universität Darmstadt, Germany
M. Gasior, CERN, Geneva, Switzerland

Abstract

Quadrupolar or beam envelope oscillations give valuable information about the injection matching and the incoherent space charge tune shift. An asymmetric capacitive pick-up was installed at GSI SIS-18 to measure these oscillations. In this contribution, we present the simulations performed to estimate the sensitivity of the quadrupolar pick-up to the beam quadrupolar moment and compare it with respect to other pick-up types installed at SIS-18. Further, dedicated beam measurements are performed to interpret the quadrupolar signal under high intensity conditions.

INTRODUCTION

A symmetric pick-up is shown in Fig. 1 along with a Gaussian beam with centroid at $\bar{x}$, $\bar{y}$ and rms dimensions $\bar{\sigma}_x$, $\bar{\sigma}_y$. The image current induced by the beam at the pick-up (PU) electrodes is derived in [1] and reproduced here,

$$J_{\text{image}}(a,\theta) = \frac{I_{beam}}{2\pi a}\Bigg\{1 + 2\left[\frac{\bar{x}}{a}\cos\theta + \frac{\bar{y}}{a}\sin\theta\right] + 2\left[\left(\frac{\bar{\sigma}_x^2 - \bar{\sigma_y}^2}{a^2} + \frac{\bar{x}^2 - \bar{y}^2}{a^2}\right)\cos 2\theta + 2\frac{\bar{x}\bar{y}}{a^2}\sin 2\theta\right] + \text{higher order terms}\Bigg\} \qquad (1)$$

On a symmetric pick-up, the four plate signals are obtained for $\theta = 0$, $\pi/2$, π and $3\pi/2$ radians. The second order component that contains beam width information is referred to as the "quadrupole moment" and is given by,

$$\kappa = \bar{\sigma}_x^2 - \bar{\sigma}_y^2 + \bar{x}^2 - \bar{y}^2 \qquad (2)$$

To extract the quadrupole moment from the pick-up electrode signals (denoted by U referring to the voltages induced), the electrodes are connected in the following "quadrupolar" configuration,

$$\begin{aligned} \Xi_q &= (U_r + U_l) - (U_t + U_b) & (3)\\ &= Z \cdot I_{beam}\left(\frac{\bar{\sigma}_x^2 - \bar{\sigma}_y^2 + \bar{x}^2 - \bar{y}^2}{a^2} + \text{higher order terms}\right) & \\ \Xi_s &= (U_r + U_l + U_t + U_b) & (4)\\ &= Z \cdot I_{beam} & \end{aligned}$$

where Z is the transfer impedance of the pick-up and Ξ_q is the quadrupolar signal and when Ξ_q is normalized to the sum signal of all electrodes Ξ_s, it is referred to as the normalized quadrupolar signal.

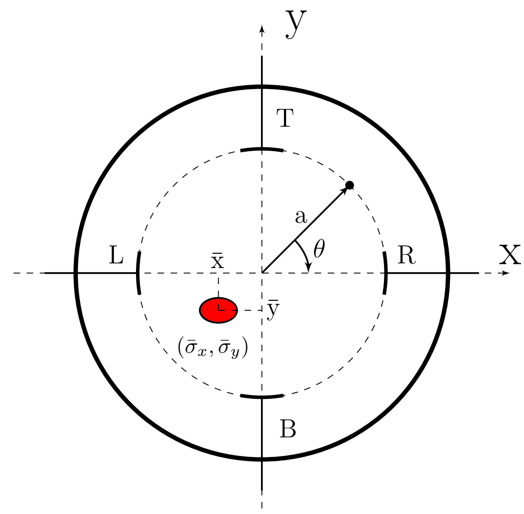

Figure 1: Symmetric pick-up for the analytical calculations.

Quadrupole signal monitors were first suggested as non-invasive emittance monitors at SLAC [1]. In synchrotrons, the quadrupole monitors were initially used to detect the injection mismatch causing envelope oscillations. It was also used to estimate the space charge dependent detuning [2] based on theoretical and numerical works [3,4]. Special pick-up designs and signal processing schemes were developed at CERN-PS to use quadrupolar pick-ups as regular emittance monitors [5].

At GSI SIS-18, quadrupolar beam transfer function (BTF) measurements were performed to get a direct measure of incoherent tune shift [6]. Due to unavailability of appropriate non-linear pick-ups int those studies, a new asymmetric pick-up was developed for SIS-18 [7]. There were recent studies which focussed on the signal processing methods to suppress the dipole contributions in the quadrupolar signal [8].

The first section of this paper summarizes the simulations performed to compare the sensitivities of various pick-up types installed at SIS-18 to the quadrupolar moment. The second section details the present installation of the quadrupolar pick-up, its data acquisition and the signal processing. The final section presents the beam experiments and results.

ISBN 978-3-95450-141-0

PICK-UP GEOMETRY AND SIMULATIONS

For the typical SIS-18 operation, the longitudinal extent of beam is much larger in comparison to the pick-up electrode length, therefore it can be well approximated by the pick-up 2D geometry and its properties can be determined electrostatically. The pick-up was simulated using the electrostatics solver in the simulation software CST EM Studio. The pick-up design used for the simulation is depicted below in Fig. 2.

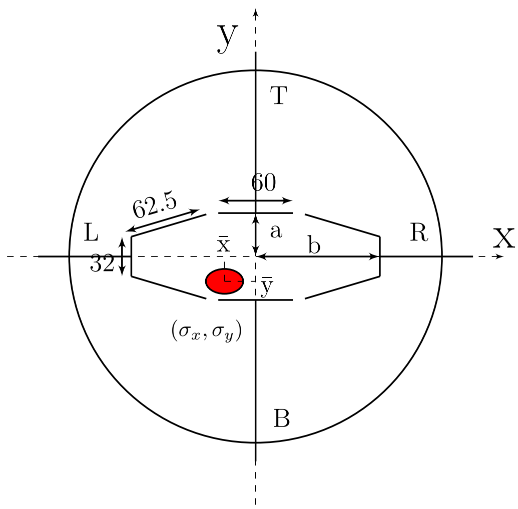

Figure 2: Front view of the pick-up design; a = 35.3 mm, b = 100.3 mm, length of the electrodes in longitudinal plane L = 216 mm [9]. All the lengths are in mm units.

In the simulation, the quadrupolar signal is obtained for each transverse horizontal beam size σ_x varying from 7.5 mm to 25 mm, while the transverse vertical beam size σ_y is kept constant at 7.5 mm. The initial values of simulated range are typical for the SIS-18 injection. The normalized quadrupolar signal Ξ calculated with CST EM Studio is shown in Fig. 3(a). It is obtained by using the difference over sum method (using Eq. 3),

$$\Xi = \frac{\Xi_q}{\Xi_s} = \frac{U_R + U_L - U_T - U_B}{U_R + U_L + U_T + U_B}$$

where U_R, U_L, U_T and U_B are defined as in the previous section.

It can be expressed as $\Xi = m_q\ (\sigma_x^2 - \sigma_y^2) + \Xi_0$, where m_q denotes the pick-up quadrupolar sensitivity and Ξ_0 is the value of the quadrupolar signal for a round and centered beam. Ξ_0 is a pick-up geometry dependent constant. $m_{q,asym} = 6.6 * 10^{-5}$ /mm^2 is determined using the linear regression method with the coefficient of determination $R^2 = 0.997$. The dipolar sensitivities for this pick-up were calculated in [9].

Comparison with Other Pick-ups

Another symmetrical pick-up is under operation in SIS-18 which is similar to the depiction in Fig. 1 with a =100 mm.

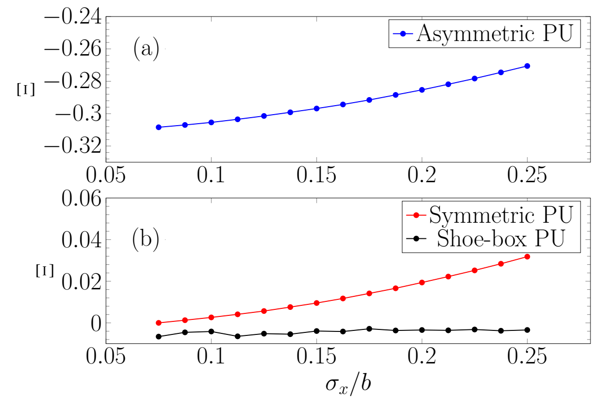

Figure 3: Quadrupole signal from the pick-ups as a function of σ_x/b; σ_y/b = 0.075, b = 100 mm.

However, it has rectangular plates with dimensions of 60 × 110 mm^2 opposed to the smaller cylindrical plates shown in Fig. 1. The sensitivity of the pick-up is calculated by the same method as for asymmetric pick-up. Figure 3(b) shows the normalized quadrupolar signal with respect to the beam dimension in the horizontal plane. The sensitivity calculated from the graph is $m_{q,sym} = 5.55 * 10^{-5}$/mm^2 with a coefficient of determination R^2 of 0.998. Similarly the sensitivity of the typical SIS-18 BPMs i.e. shoe-box pick-ups [10] is also calculated as $m_{q,sb} \approx 0$ from the graph shown in Fig. 3(b). The shoe-box pick-ups are optimized for linear response to change in the beam position, thus all the higher order components including the quadrupolar terms are strongly suppressed. The transfer impedance (Z) of the mentioned pick-ups roughly scale with their lengths and are calculated for a relativistic beam i.e. $\beta \approx 1$ as $Z_{asym} \approx 19\,\Omega$, $Z_{sym} \approx 13\,\Omega$ and $Z_{sb} \approx 7\,\Omega$.

The asymmetric pick-up (shown in Fig. 2) proves to be a good option to be used a quadrupolar pick-up due to 20% higher sensitivity compared to symmetric pick-up as well as high transfer impedance. The shoe-box BPMs which are used as beam position monitors (BPM) at SIS-18 are not sensitive to the quadrupolar moment at all.

DATA ACQUISITION AND SIGNAL PROCESSING

The signals from the asymmetric pick-up (shown in Fig. 2) are individually connected to diode based peak detectors [11]. The peak detectors strongly suppress the common mode due to the monopolar component of the beam signal. The time constant of the peak detector plays an important role in the common mode suppression. The outputs of the peak detectors from the opposite plates are added using passive power combiner. The output of each of these combiners are connected to a differential amplifier, such that "quadrupole configuration" Eq. 3 is obtained. This ensures effective suppression of the dipolar signal. The resulting signal is amplified by 45 dB and low pass filtered with a 3 dB cut-off of ≈ 1 MHz.

The minimum detectable quadrupole moment oscillations of the beam can be estimated by the noise model of the peak detectors and the amplifiers. A full derivation of a comparable system can be found in [11]. The measured output noise from the amplifiers after the default gain of 45 dB is 0.6 mV rms. The quadrupolar sensitivity of the asymmetric pick-up was calculated as $m_{q,asym} = 6.6 * 10^{-5}$ /mm^2 and transfer impedance $Z_{asym} = 19\ \Omega$ in the previous section. For a beam current of $I_{beam} = 1$ mA and a quadrupolar moment κ oscillation of amplitude 0.01 mm^2 p-p, the quadrupole signal amplitude after 45 dB amplification is,

$$\Xi_q = Z_{asym} * I_{beam} * m_{asym} * \kappa * 180 = 40\ \mu\text{V p-p} \quad (5)$$

Thus, the quadrupolar moment oscillation of amplitude 0.1 mm^2 p-p for a 1 mA beam current can be detected from the power spectral density of 512 turn-by-turn quadrupolar signal with a signal to noise ratio of 6 dB. One should note that the quadrupolar signal is not normalized to the beam intensity.

INTERPRETATION OF THE QUADRUPOLAR PICK-UP SIGNAL

The quadrupolar signal was measured for various beam intensity levels. Due to unavailability of a suitable quadrupolar exciter during these measurements, we utilized the injection mismatch to "excite" the beam size oscillations.

Injection Mismatch and Beam Oscillations

Injection mismatch is undesired in general since it leads to beam emittance dilution [12]. There are various sources of beam mismatch during injection.

1. If the beam phase space has a different orientation with respect to synchrotron twiss parameters at its injection point, the beam is said to have a "beta" mismatch. The beta mismatch leads to coherent envelope oscillations in the plane of mismatch at approximately twice the tune frequency (explained later in this section) [3, 4].

2. If the beam is not injected on the closed orbit, there is a position mismatch leading to oscillations at the betatron tune frequency (Q_x, Q_y).

3. Another source of mismatch is the dispersion at the point of injection, leading to beam size oscillations at the tune frequency [13].

The multi-turn injection in the horizontal plane at GSI SIS-18 leads to an inherently mismatched beam in the horizontal plane leading to a combination of various mismatches and all of them contribute to the quadrupolar moment of the beam. The resulting coherent oscillations are usually "Landau" damped due to frequency spread in a few hundred turns.

If the beam position and envelope is oscillating due to the injection mismatch, the quadrupolar moment in Eq. 2 obtains a time dependence,

$$\kappa(t) = {\sigma_x}^2(t) - \sigma_y^2(t) + x^2(t) - y^2(t) \quad (6)$$

While expanding Eq. 6, we perform the following simplifications,

- We consider only the even modes for an anisotropic beam [4] since the sensitivity of the quadrupolar pick-up oriented with the beam pipe is very reduced for the odd (or coupled) modes.
- The contribution caused by dispersion to the beam size is negligible compared to that of beam emittance, therefore we ignore the dispersion mismatch component.
- The frequency spread in the beam which leads to decoherence of beam oscillations is also ignored.

Figure 4 shows the beam position and beam envelope variation for a KV beam at two time instants.

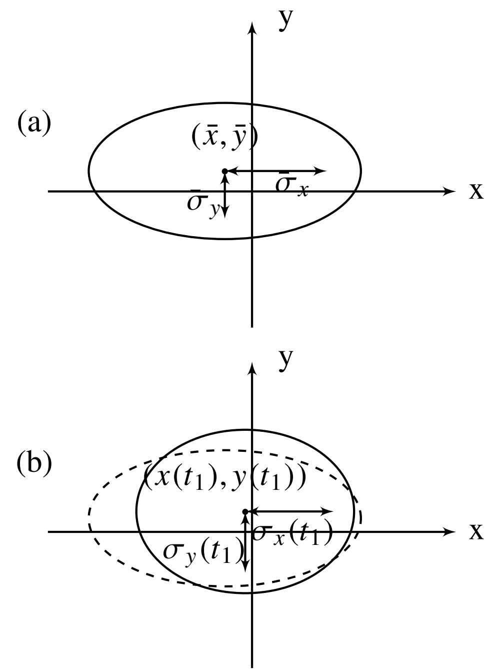

Figure 4: (a) Schematic showing the transverse profile of a stationary KV beam. (b) Schematic showing the excited beam at an arbitrary time t_1 performing beam position and envelope oscillations in both planes in comparison with the initial state (dashed).

If the initial beam position oscillation amplitudes are given by a_x and a_y, and beam envelope oscillation amplitudes are given by a_{xx} and a_{yy}, the time dependence of beam position and beam size can be written as,

$$\begin{aligned} \sigma_x(t) &= \bar{\sigma}_x + a_{xx}\cos(2\pi Q_{coh,1} t) \\ \sigma_y(t) &= \bar{\sigma}_y + a_{yy}\cos(2\pi Q_{coh,2} t) \\ x(t) &= \bar{x} + a_x \cos(2\pi Q_x t) \\ y(t) &= \bar{y} + a_y \cos(2\pi Q_y t) \end{aligned} \quad (7)$$

ISBN 978-3-95450-141-0

Substituting Eqs. 7 into Eq. 6 and ignoring second order terms of beam envelope oscillations, we obtain,

$$\begin{aligned}\kappa(t) &= \bar{\sigma}_x^2 + 2\bar{\sigma}_x a_{xx}\cos(2\pi Q_{coh,1}t) - \bar{\sigma}_y^2 \\ &\quad - 2\bar{\sigma}_y a_{yy}\cos(2\pi Q_{coh,2}t) + \bar{x}^2 + 2\bar{x}a_x\cos(2\pi Q_x t) \\ &\quad + \frac{{a_x}^2}{2}(1+\cos(2\pi 2Q_x t)) - \bar{y}^2 - 2\bar{y}a_y\cos(2\pi Q_y t) \\ &\quad - \frac{{a_y}^2}{2}(1+\cos(2\pi 2Q_y t)) \qquad (8)\end{aligned}$$

The frequency of the even coherent quadrupolar modes ($Q_{coh,1}$,$Q_{coh,2}$) for a KV beam is given by [6],

$$\begin{aligned}Q_{coh,1} &= 2Q_{x0} - (1.5 - 0.5\frac{\sigma_x}{\sigma_x+\sigma_y})\Delta Q_{sc,x} \\ Q_{coh,2} &= 2Q_{y0} - (1.5 - 0.5\frac{\sigma_y}{\sigma_x+\sigma_y})\Delta Q_{sc,y} \qquad (9)\end{aligned}$$

Under no space charge conditions, $Q_{coh,1} = 2Q_{x0}$ and $Q_{coh,2} = 2Q_{y0}$ where Q_{x0}, Q_{y0} are the low intensity tunes or the "bare" tunes of the synchrotron. The coherent betatron tune Q_x, Q_y of a coasting beam are shifted due to dipolar wall impedances given by $\Delta Q_{coh(x,y)}$. The coherent tune is not directly affected by space charge. The coherent tune shifts ΔQ_{coh} for a coasting beam at injection in SIS-18 are negligible compared to incoherent tune shifts ΔQ_{sc} [14], therefore we assume $Q_x \approx Q_{x0}$ and $Q_y \approx Q_{y0}$.

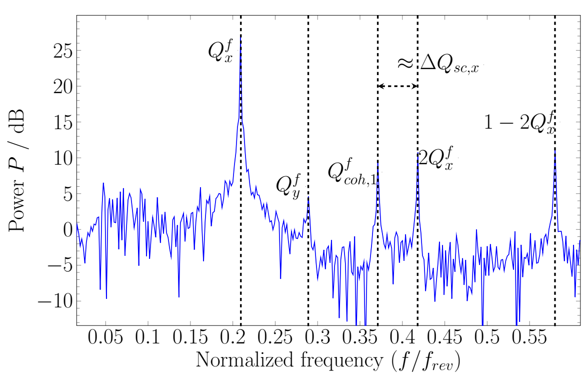

Figure 5: Typical spectrum of the quadrupolar signal for a high intensity beam immediately after injection with $I_{beam} \approx 6$ mA and other parameters given in Table 1.

Figure 5 shows an example of the baseband spectra of the quadrupolar signal for $I_{beam} \approx 6$ mA and other parameters given in Table 1. The horizontal axis shows the measured frequencies normalized to revolution frequency f_{rev}. The superscript in Q_x^f denotes fractional part of horizontal tune. In the spectra, frequency peaks expected from Eq. 8 are clearly seen. The presence of horizontal and vertical tunes suggest position mismatch in both planes. A peak at twice the horizontal tune is also clearly seen. Only one of the coherent envelope oscillation modes ($Q_{coh,1}$) is visible suggesting that the beam was well "beta" matched in the vertical plane. The spacing between $Q_{coh,1}$ and $2Q_x^f$ peaks is approximately the incoherent tune shift in horizontal plane ($\Delta Q_{sc,x}$) as expected by Eq. 9.

Experiments

Careful measurements were performed to see a systematic effect of beam intensity on the quadrupolar signal spectrum. The current was increased in steps from the UNILAC without affecting the parameters of SIS-18 multi-turn injection, and the frequency spectrum of the quadrupolar signals were recorded at several intensities. Table 1 shows the important beam parameters.

Table 1: Measured Parameters for N^{7+} Beam Experiment

Parameters	Value
W_{kin} (MeV/u)	11.45
I_{beam} (mA)	$\approx 0.6 - 6$
$\varepsilon_x, \varepsilon_y (2\sigma)$ (mm-mrad)	32,51
Q_{x0}, Q_{y0}	4.21,3.3

The beam profile measurements were performed in parallel using the Ionization profile monitor (IPM). The measured beam profiles were found to be independent of the current level. The incoherent space charge tune shift can be estimated using the beam parameters,

$$\Delta Q_{sc} = \frac{qI_{beam}R}{2\pi\epsilon_0 c W_0 {\gamma_0}^2 \beta_0^3(\varepsilon_x + \sqrt{\varepsilon_x\varepsilon_y\frac{Q_{x0}}{Q_{y0}}})} \qquad (10)$$

with $\varepsilon_x, \varepsilon_y$ as the rms emittance of the equivalent K-V distribution, q the particle charge and $W_0 = \gamma_0 m_0 c^2$ the rest energy, γ_0 and β_0 are the relativistic parameters and R is the synchrotron radius.

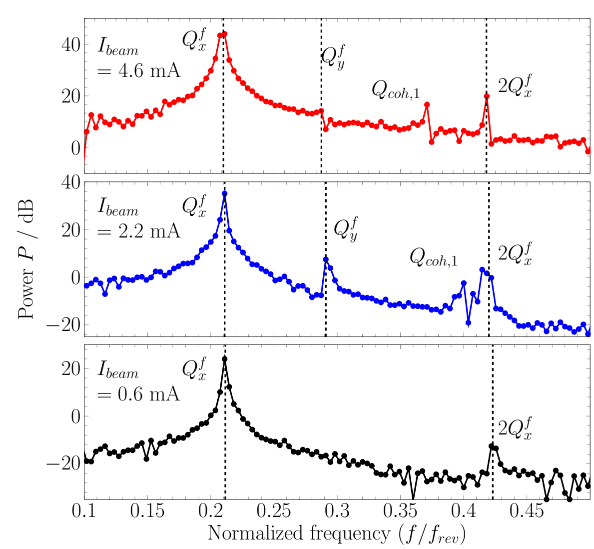

Figure 6: Shift of coherent quadrupole mode $Q_{coh,1}$ with beam current.

Figure 6 shows the spectrum at three intensities. For lowest intensity (Fig. 6 bottom), the calculated $\Delta Q_{sc,x}$ using Eq. 10 is ≈ 0.004, and the $Q_{coh,1}$ is difficult to distinguish from the $2Q_x^f$ line. Thus, we are unable to resolve the beam position and beam envelope oscillations. As the current is increased to 2.2 mA (Fig. 6 middle), the component resulting from beam size oscillations i.e $Q_{coh,1}$ separates from the $2Q_x^f$ peak and moves toward lower frequency as predicted by Eq. 9.The $\Delta Q_{sc,x}$ calculated is 0.017 in this case and roughly corresponds to the frequency shift. On further increase of beam current i.e. I_{beam} = 4.6 mA (Fig. 6 top), the $Q_{coh,1}$ peak moves further as a function of $\Delta Q_{sc,x}$ which is calculated to be 0.037. This procedure can be used as a direct method to measure ΔQ_{sc}.

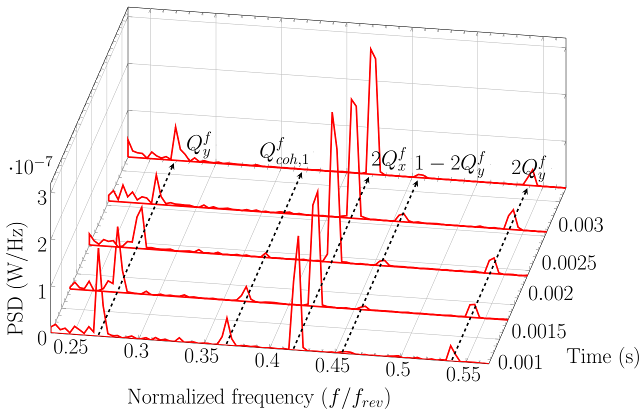

Figure 7: Quadrupolar signal spectra from Fig. 6 (top) over time. The quadrupolar mode $Q_{coh,1}$ damps much faster than the corresponding dipolar mode $2Q_x^f$.

The waterfall plot in Fig. 7 shows the evolution of frequency spectra over time immediately after injection. The first spectra is the same as the spectra in Fig. 6 for I_{beam} = 4.6 mA. The quadrupolar mode damps in $\approx$ 1 ms which corresponds to $\approx$ 200 turns at injection. One can note that the position related oscillations resulting in peaks at Q_y^f, $2Q_y^f$ and $2Q_x^f$ sustain for at least until 1000 turns, which hint towards a weaker damping mechanism against these oscillations.

SUMMARY AND OUTLOOK

The asymmetric pick-up installed at SIS-18 was simulated and compared with other installed pick-ups in terms of the quadrupolar sensitivity. Peak detectors were used to suppress the common mode signal, and pick-up electrode signals were connected in quadrupolar configuration to suppress the dipolar signal. This followed by low noise amplifier made our measurements very sensitive to coherent quadrupolar moment oscillations. Coherent quadrupolar oscillations were excited due to injection mismatch, and a clear correlation of the quadrupolar mode frequency shifts with the space charge tune shift was observed. Direct measurement of space charge tune shift by this method will be used to optimize the machine working point such that coherent dipole or quadrupole modes do not encounter any strong machine resonances. It can also be used as a diagnostic for efficient injection matching. Further work concerning installation of a quadrupolar exciter at SIS-18 is foreseen.

ACKNOWLEDGEMENT

We would like to emphasize the contribution of P. Moritz, who passed away on September 19th, 2014. The asymmetric pick-up used in this contribution is just one among his numerous scientific and technical developments, which are being continuously and successfully used at GSI.

REFERENCES

[1] R. Miller et al., "Non invasive emittance monitor", PAC'83, Washington, 1983.

[2] M. Chanel et al., "Study of beam envelope oscillations by measuring the beam transfer function with quadrupolar pick-up and kicker", EPAC'96, Sitges, 1996.

[3] W. Hardt, "On the incoherent space charge limit for elliptic beams", CERN/ISR/Int. 300 GS/66.2.

[4] I. Hofmann, "Stability of anisotropic beams with space charge", Physical Review E 57 (4), 4713.

[5] A. Jansson et al., "Noninvasive single-bunch matching and emittance monitor", Phys. Rev. ST Accel. Beams 5, 072803.

[6] R. Baer et al., "Measurement of space-charge-induced frequency shifts of quadrupolar beam oscillations in the SIS", NIM-A 415 460—463, 1998.

[7] Private communication with P. Moritz, GSI.

[8] J.A.Tsemo Kamga et al., "New method for reducing the contribution of the beam position in the quadrupolar signal", GSI Scientific report 2012.

[9] J. Latzko et al., "Simulations of the position sensitivity for SIS18 capacitive BPM with non-standard geometry", GSI scientific report 2013.

[10] P. Kowina et al., "Optimization of "Shoe-box type" beam position monitors using the finite element methods", DIPAC 2005, Lyon, France.

[11] M. Gasior et al., "The principle and first results of betatron tune measurement by direct diode detection", LHC-Project-Report-853 ; CERN-LHC-Project-Report-853, 2005.

[12] M.J Syphers et al., "Injection mismatch and phase space dilution", FNAl report, FN-458, 1987.

[13] M. Minty et al., "Injection envelope matching in storage rings", Proc. 1995 Part. Acc. Conf. and Intl. Conf. on High Energy Accel (Dallas, TX, 1995) 536.

[14] R. Singh et al., "Interpretation of transverse tune spectra in a heavy-ion synchrotron at high intensities", Phys. Rev. ST Accel. Beams 16, 034201, 2013.

ISBN 978-3-95450-141-0